

Design of multi-wing chaotic systems with higher largest Lyapunov exponent

Shilalipi Sahoo*, Binoy Krishna Roy

Department of Electrical Engineering, National Institute of Technology Silchar, Silchar 788010, Assam, India



ARTICLE INFO

Article history:

Received 30 July 2021

Revised 4 February 2022

Accepted 15 February 2022

Available online 24 February 2022

Keywords:

Multi-wing chaotic attractor

Nonlinear function

Largest Lyapunov exponent

Chaotic systems

ABSTRACT

A multi-wing chaotic attractor with higher value of the largest Lyapunov exponent is more useful for its practical applications. This paper proposes a new design technique to generate multi-wing chaotic attractors from two-wing chaotic attractors, available in the literature. The Chen and the Lu systems are considered for demonstration. A nonlinear term of the original system is multiplied by a nonlinear function to generate multi-wings attractors. The number of wings is changed by varying the number of equilibrium points, and the equilibrium points are changed by varying the parameters of the newly added nonlinear function. The new multi-wing chaotic systems have a higher value of the largest Lyapunov exponent than their respective original systems. An interesting behavior is observed in the proposed system, i.e., the largest Lyapunov exponent increases with the variation of a system parameter. Further, the largest Lyapunov exponents of the new systems are much higher than some similar available papers.

© 2022 Elsevier Ltd. All rights reserved.

1. Introduction

Chaos theory has a widespread application starting from the field of mathematics to the field of biology. The most recent pandemic, i.e., the outbreak of COVID-19 is also modelled as a chaotic system [1]. The development, design and analyses of chaotic systems to explore new characteristics and their real-life applications have been gaining interest among the researchers. There are different kinds of chaotic attractors like multi-torus [2], multi-cavity [3], multi-wing, chaotic attractors with multi-stability and mega-stability [4], etc. However, complex dynamics of multi-wing chaotic attractors attract the interest of researchers in this area.

In the past two decades, a significant number of multi-wing chaotic systems with intricate dynamics have been reported. Hidden multi-wing and multi-scroll attractors [5], hidden multi-wing in a hyperchaotic system [6–8], multi-scroll attractor with an infinite number of equilibria, hyperchaotic multi-wing [9], 4-D chaotic system with 2-wing, 4-wing and coexisting attractors [10], fractional-order multi-wing chaotic systems [11,12]. Again, coexistence of multiple multi-scroll chaotic attractors is observed in a memristor-based chaotic system [13]. These multi-wing chaotic attractors with enhanced complexity have become more suitable for different chaos-based applications such as secure communication [14,15], image-encryption [16], cryptanalysis [17], etc.

The key design feature considered in most of the multi-wing chaotic systems is to change the number of equilibrium points and their natures. The nature of equilibrium points plays a vital role in the generation of multi-wings. A saddle focus of index-2 helps in the generation of a wing. A multi-segment even-symmetric nonlinear function is used to generate multi-wings in Zhou et al. [8], Tang et al. [18], Zhou et al. [19]. With the help of this nonlinear function, the number of equilibria with saddle focus of index-2 is changed to generate the desired number of wings. Also, by replacing an absolute function with a saw-tooth function in the above mentioned nonlinear function, multi-wings are generated in Yu et al. [20]. Another approach is followed in Hong et al. [21, 22], where a pulse excitation is used to generate $(2N + 1)$ -scroll attractor. Further, multi-wings are obtained using the translation transformation principle [23]. In this technique, a stair-case function is introduced to design multi-scroll and multi-wing chaotic systems, Liu et al. [23], Wang et al. [24], Chen et al. [25]. Moreover, hyperbolic sine function [26], signum function [27] and tan-hyperbolic function [28] are used to create multi-wing attractors. A multi-wing chaotic system [29] is designed from a robust chaotic system by modifying the position and amplitude parameters of the system. In [30], a 3D $n \times m \times l$ -grid multi-wing chaotic attractor is obtained using a three-step procedure. Similarly, a 2D grid of scroll attractors is constructed using a cellular nonlinear network [31]. One state variable of the Lorentz system is replaced by a piece-wise hysteresis function to generate a grid multi-wing butterfly chaotic system in Huang et al. [32]. Reference [33] describes a nonlinear coupling method to generate a grid multi-wing from the Lorentz system.

* Corresponding author.

E-mail address: shilalipi_rs@ee.nits.ac.in (S. Sahoo).

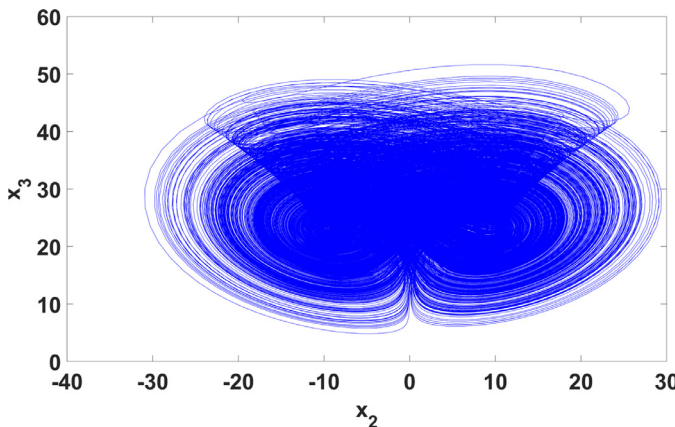


Fig. 1. Two-wings attractor of the Chen system.

Zhang et al. reported a 4-D hyperchaotic system [34], which can generate $n \times m$ -wings attractor. Again, Wu et al. presented two different pulse control methods to get multi-butterfly attractors from Sprott-C system [35].

Based on the above-discussed status of the literature, this paper proposes a new design technique to create a multi-wing chaotic attractor from a two-wing chaotic system. A nonlinear function having sine term is added to the Chen system for this purpose [36]. Then the parameters of the same function act as the control parameter to change the number of wings. By using the proposed method, along with number of wings, the magnitude of the largest Lyapunov exponent (LLE) is also increasing. The proposed technique is also tested for the Lu chaotic system. These newly designed chaotic systems have much higher largest Lyapunov exponents than the LLE in some similar papers reported in the literature. A large magnitude of LLE indicates the highly intricate nature of the system dynamics. The details are described in the subsequent sections.

The organisation of the paper is as follows. After introduction, Section 2 deals with the design of a new multi-wing chaotic system. Dynamical properties of the new multi-wing chaotic system are discussed in Section 3. Results and Discussion are taken up in Section 4. In Section 5, the applicability of the proposed design approach is tested for the Lu system. Finally, in Section 6, conclusions of the paper are drawn.

2. Design of a new multi-wing chaotic system

The proposed design approach introduces a new nonlinear function to an available two-wing chaotic system. The nonlinear function is $f(x) = (1 - k \sin(k_1 x))$, where k and k_1 are the two parameters used, respectively, to control the signal amplitude and frequency, and x is the state variable. The new nonlinear function is multiplied with a nonlinear term of the system equation. The number of equilibrium points of the modified system is changed with the variation of k_1 . This in turn changes the number of wings of a chaotic attractor.

The state equations of the original Chen System [36] are reproduced below.

$$\begin{cases} \dot{x} = a(y - x) \\ \dot{y} = cy - xz + (c - a)x \\ \dot{z} = -bz + xy \end{cases} \quad (1)$$

With $a = 35$, $b = 3$, $c = 28$, there is a two-wing attractor in System (1), as shown in Fig. 1.

Multi-wing chaotic attractors are more complex in nature compared with two-wing attractors. Hence, to generate a multi-wing attractor, a nonlinear function is introduced in the original Chen

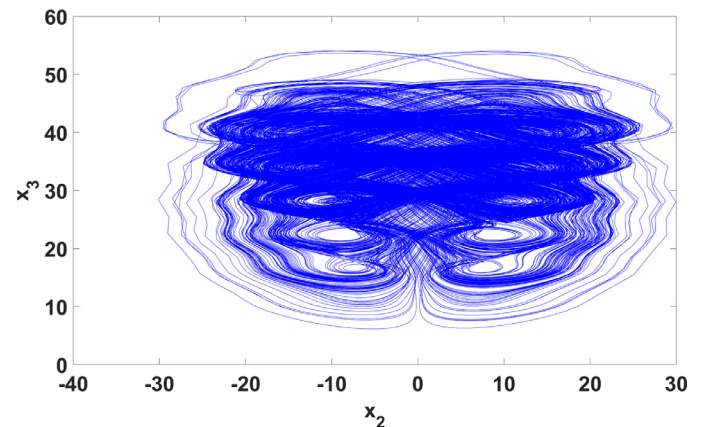


Fig. 2. 10-wings chaotic attractor of the new modified Chen system.

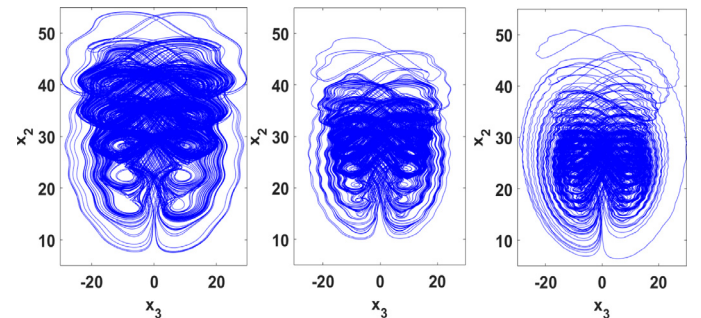


Fig. 3. Number of wings increases with the increasing value of k_1 in $x_2 - x_3$ plane, from left $k_1 = 1$, $k_1 = 2$, $k_1 = 4$.

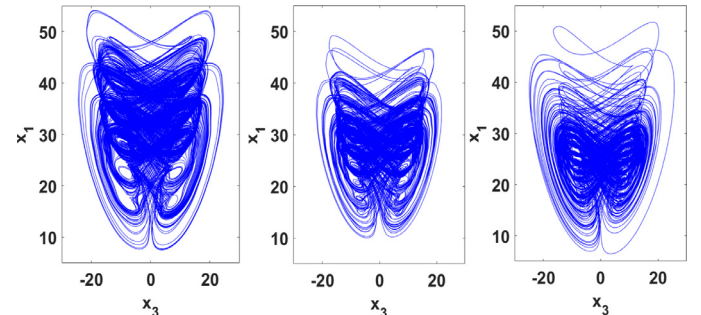


Fig. 4. Number of wings increases with the increasing value of k_1 in $x_1 - x_3$ plane, from left $k_1 = 1$, $k_1 = 2$, $k_1 = 4$.

system [36]. The modified Chen system is shown in (2).

$$\begin{cases} \dot{x} = a(y - x) \\ \dot{y} = cy - xz(1 - k \sin(k_1 z)) + (c - a)x \\ \dot{z} = -bz + xy \end{cases} \quad (2)$$

The parameters a , b and c are the same as that of the original Chen system and $k = 0.5$ is considered. Using the above said design procedure, a 10-wing chaotic attractor is obtained with $k_1 = 1$, and is shown in Fig. 2. In this newly designed system, k_1 is the control parameter. The impact of k_1 in the generation of multi-wings is shown in Figs. 3 and 4. The values of k_1 are 1, 2 and 4. Multi-wings are obtained with an arbitrary initial condition of $[1, 0, 3]^T$. These results are obtained using ode45 solver with observation time of 2000 s and a step size of 0.005 s.

3. Dynamical properties of the new multi-wing chaotic system

Various dynamical characteristics of the proposed multi-wing chaotic system are discussed in this section.

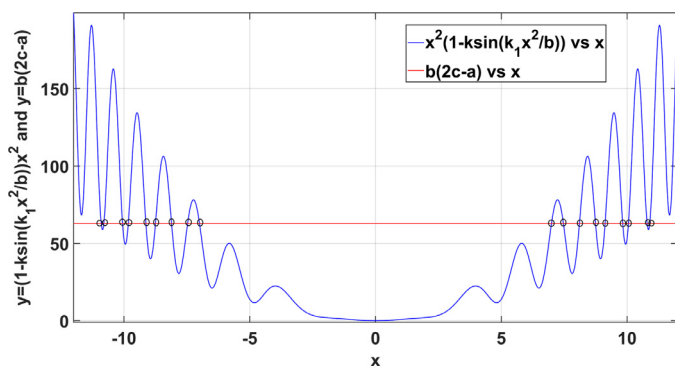


Fig. 5. Plot to calculate the equilibrium points of System (2) with $k = 0.5$ and $k_1 = 1$.

3.1. Equilibrium points and their nature

The equilibrium points of the new multi-wing chaotic system in (2) are calculated by equating the derivative of states to zero and are given in (3).

$$\begin{cases} a(y - x) = 0 \\ cy - xz(1 - k \sin(k_1 z)) + (c - a)x = 0 \\ -bz + xy = 0 \end{cases} \quad (3)$$

The solution of Eq. (3) results $y = x$, $z = \frac{x^2}{b}$, and $x^2(1 - k \sin(\frac{k_1 x^2}{b})) = b(2c - a)$. Here, x is obtained graphically using the plot shown in Fig. 5.

We find that there are 18 equilibria as labelled by small circles in Fig. 5. These equilibrium points are $(\pm 7, \pm 7, 16.33)$, $(\pm 7.46, \pm 7.46, 18.55)$, $(\pm 8.1, \pm 8.1, 21.87)$, $(\pm 8.74, \pm 8.74, 25.46)$, $(\pm 9.12, \pm 9.12, 27.725)$, $(\pm 9.84, \pm 9.84, 32.275)$, $(\pm 10.06, \pm 10.06, 33.734)$, $(\pm 10.8, \pm 10.8, 38.88)$, $(\pm 10.9, \pm 10.9, 39.603)$.

We need to find the nature of the above equilibrium points. The Jacobian of System (2) is given below.

$$J = \begin{bmatrix} -a & a & 0 \\ (c-a) - z(1 - k \sin(k_1 z)) & c - x + kx(\sin(k_1 z) + k_1 z \cos(k_1 z)) & x \\ y & x & -b \end{bmatrix}$$

The eigenvalues corresponding to these equilibrium points are calculated and the outcomes reveal that there are 10 equilibria with saddle focus of index-2. These eigenvalues are $(-28.6596, 9.3298 \pm j 29.3343)$, $(-33.9691, 11.9845 \pm j 38.073)$, $(-36.3909, 13.1954 \pm j 42.824)$, $(-37.4803, 13.74 \pm j 45.8257)$, $(-34.444, 12.22 \pm j 39.2742)$. Due to these 10 saddle focus of index-2 equilibria, a 10-wing attractor is generated [18,20,25,36]. Further, according to the Homoclinic Silnikov Theorem, each saddle-focus equilibrium with index 2 can generate a unique wing.

3.2. Dissipativity

The dissipative nature of a system is determined from the sign of its divergence. The divergence of System (2) is given by

$$\frac{\partial \dot{x}}{\partial x} + \frac{\partial \dot{y}}{\partial y} + \frac{\partial \dot{z}}{\partial z} = c - (a + b) \quad (4)$$

For a set of parameters, the system will be dissipative when $(a + b) > c$. System (2) is dissipative for the chosen set of parameters. Thus, the volume of system trajectories will converge to zero as $t \rightarrow \infty$.

3.3. Lyapunov exponents and Lyapunov dimension

The Lyapunov exponents are the only quantitative measure to ensure whether the system is chaotic or not. The Lyapunov

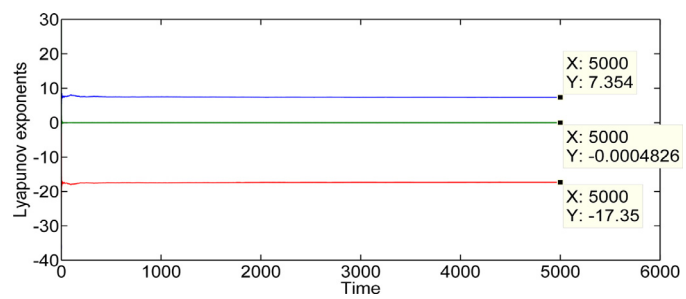


Fig. 6. Lyapunov exponents of the new multi-wing Chen system.

exponents are calculated for a long observation time of 5000 sec and with a step size 0.01 sec. The Lyapunov exponents are 7.354, 0, -17.35. The time history of the Lyapunov exponents of System (2) is shown in Fig. 6. The $(+, 0, -)$ nature of the Lyapunov exponents confirms the chaotic nature of the proposed new system [37]. The Lyapunov exponents are calculated using the Wolf algorithm. It may be noted that the largest Lyapunov exponent of the proposed system (7.354) is comparatively much higher than that of the original Chen system (2.022). Therefore, the proposed system is comparatively more chaotic [38].

The Lyapunov dimension of the new chaotic system is calculated as

$$D_L = j + \frac{\sum_{i=1}^j LE_i}{|LE_{j+1}|} = 2.424, \quad (5)$$

with usual notations. Therefore, the fractal dimension of 2.424 confirms the chaotic nature of System (2).

4. Results and discussion

The original Chen system generates a two-wing attractor with $a = 35$, $b = 3$, $c = 28$. A nonlinear function $(1 - k \sin(k_1 z))$ is multiplied with the nonlinear term of the second state equation. Thus, a multi-wing chaotic attractor is generated, as shown in Fig. 2. The value of parameters a , b , c of the modified Chen system are the same as that of the original Chen system, and $k = 0.5$, $k_1 = 1$ are considered. This set of parameters has resulted a 10-wing attractor, as seen in Fig. 2. The comparatively higher largest Lyapunov exponent of the modified Chen system confirms more chaotic nature of the proposed system. The effect of variation of k_1 is seen in Figs. 3 and 4. In these two figures, it is shown that the number of wings of the chaotic attractor is increasing with an increase in value of k_1 .

According to the Homoclinic Silnikov theorem, each saddle-focus equilibrium with index 2 can generate a unique wing [18,20,25,36]. Now, we analyse what happens to the number of equilibrium points of the new system when k_1 value is increased? The solution can be visualised in Fig. 7 for $k_1 = 2$ and in Fig. 8 for $k_1 = 4$. The number of equilibrium points with saddle focus of index-2 is calculated, and the number of possible multi-wings is observed from the corresponding chaotic attractors for different values of k_1 . The details are shown in Table 1.

In the proposed multi-wing Chen chaotic system, the number of wings is changing with the variation in k_1 . With the increasing value of k_1 from 1 to 8, there is a slight change in the amplitude of the chaotic attractors but a considerable increment in the number of wings. Naturally, the distance between consecutive wings decreases gradually with the increasing value of k_1 . When a magnified version of the attractor for $k_1 = 8$ (Fig. 9) is considered, the wings of the multi-wing chaotic attractor can be seen more clearly. Our limitation may be to display the attractor in an appropriate size to observe all the wings.

Table 1
Effect of k_1 in the generation of wings and number of equilibrium points.

k_1	Total no. equilibrium points(EPs)	Number of saddle focus of index-2 EPs	Number of possible multi-wings
1	20	10	10
2	38	20	20
4	70	36	36
8	142	72	72

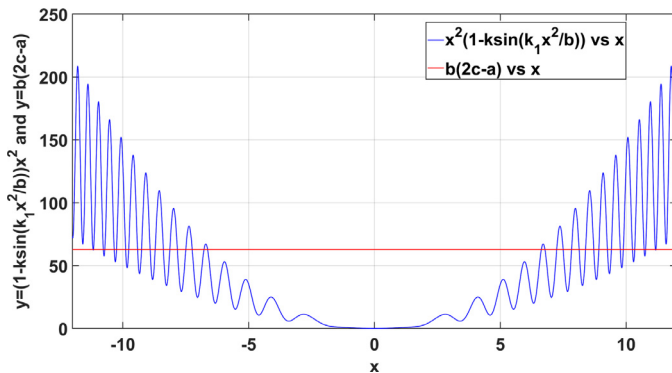


Fig. 7. Equilibrium points of System (2) with $k_1 = 2$.

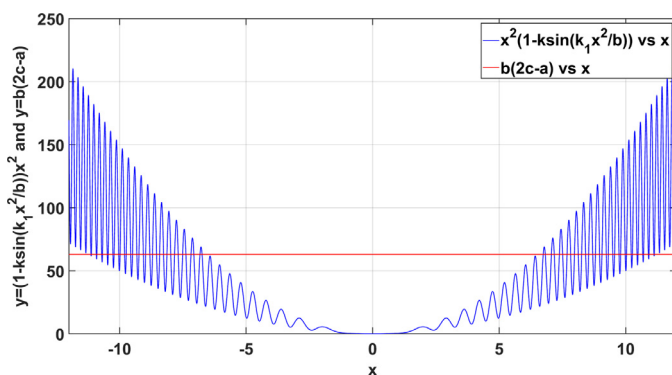


Fig. 8. Equilibrium points of System (2) with $k_1 = 4$.

Further, when higher values of k_1 are considered, there is an increase in both the number of equilibrium points and the saddle focus of index-2 nature of equilibrium points. The enhancement in the saddle focus of index-2 equilibrium points suggests the presence of more multi-wings. However, multi-wings are not visible for higher values of k_1 . For example $k_1 = 100, 500, 1000$, phase portraits are shown in Fig. 10. Hence, the chaotic attrac-

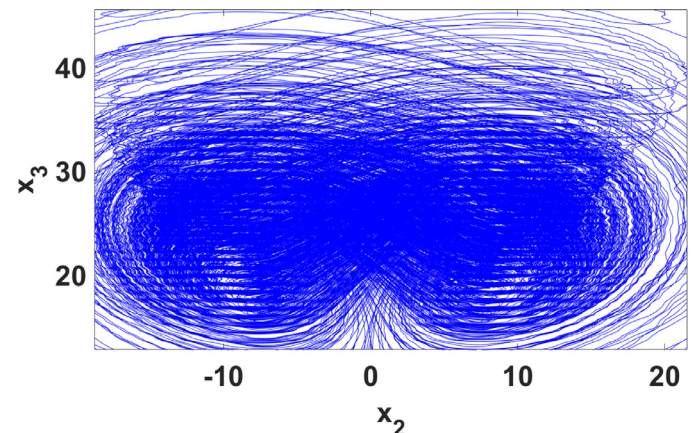


Fig. 9. Magnified version of the multi-wing chaotic attractor of System (2) for $k_1 = 8$.

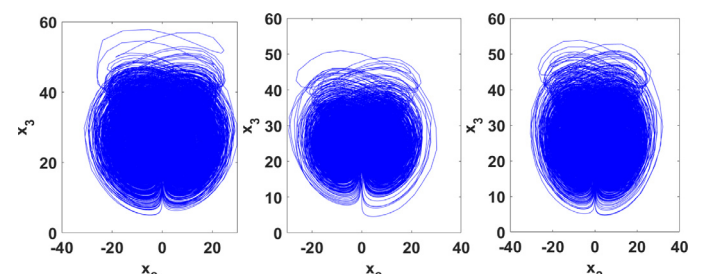


Fig. 10. Phase portraits are plotted for higher values of k_1 in $x_2 - x_3$ plane, from left $k_1 = 100, k_1 = 500, k_1 = 1000$.

tors obtained for higher values of k_1 can be termed as “pseudo-multi-wing” chaotic attractors. However, for lower values of k_1 , the number of multi-wings is equal to the number of equilibrium points with a saddle focus of index-2. Hence, the multi-wings generated up to $k_1 = 8$ can be considered an actual multi-wing attractor. For a higher $k_1 > 8$, the generated multi-wings may be termed as pseudo-multi-wing attractors.

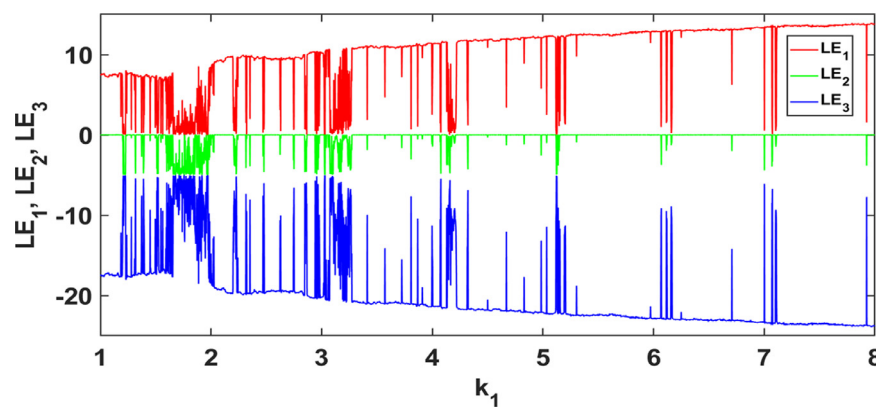


Fig. 11. Lyapunov spectrum of System (2) with k_1 from 1 to 8.

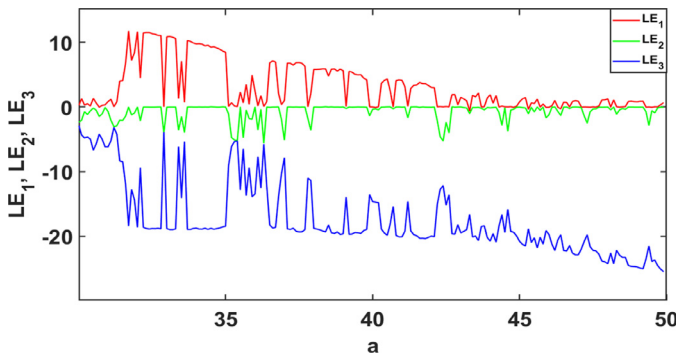


Fig. 12. Lyapunov spectrum of System. (2) with respect to a , where a is varied from 30 to 50 and k_1 is taken as 2.

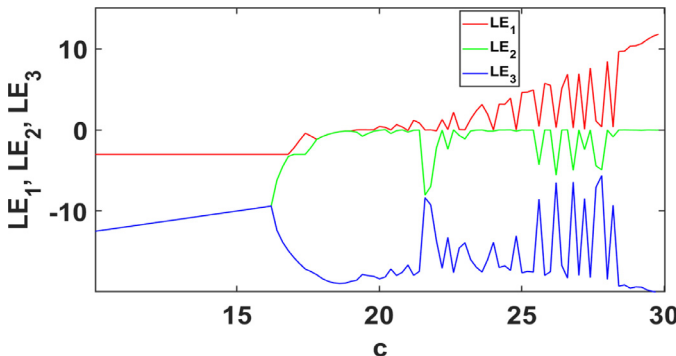


Fig. 13. Lyapunov spectrum of System. (2) with respect to c , and c is varied from 10 to 30 and k_1 is taken as 2.

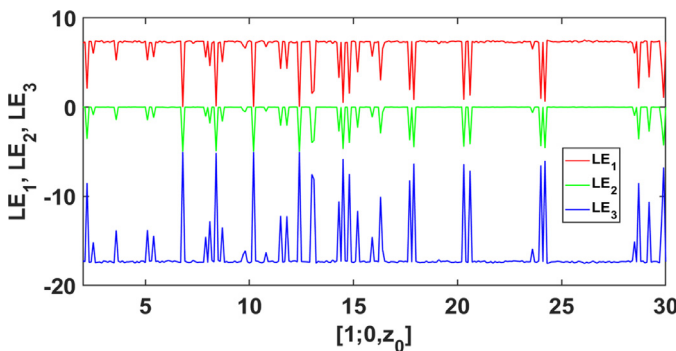


Fig. 14. Lyapunov spectrum of the new multi-wing Chen system with initial condition $[1;0;z_0]$, where z_0 is varied from 2 to 30 and other parameters are same with that of System (2).

Lyapunov spectrum of System (2) with respect to different parameters are plotted. Figs. 11–14 present the Lyapunov spectrum of the proposed modified Chen system with respect to k_1 , a , c and initial condition $[1; 0; z_0]$ respectively. In Fig. 11, k_1 is varied from 1 to 8 and the outcome of this figure confirms that the largest LE increases with the increase value of k_1 . Thus, the proposed modified Chen system exhibits more chaoticness with higher value of k_1 . This property makes the designed system more suitable for chaos-based applications.

In addition to the Lyapunov spectra, bifurcation diagrams are plotted with respect to parameter k_1 in Figs. 15–17 to have an in-depth analysis of various behaviours of System (2). From the bifurcation diagrams, it is observed that there is a large chaotic region from $k_1 = 1$ to $k_1 = 8$ and also, the width of the periodic windows is gradually decreasing with increasing value of k_1 . Further, it is

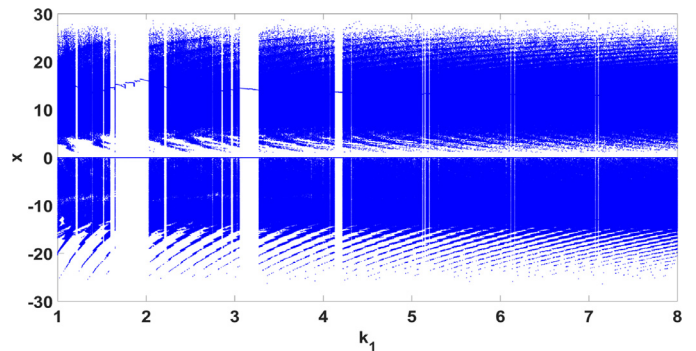


Fig. 15. Bifurcation diagram x vs. k_1 .

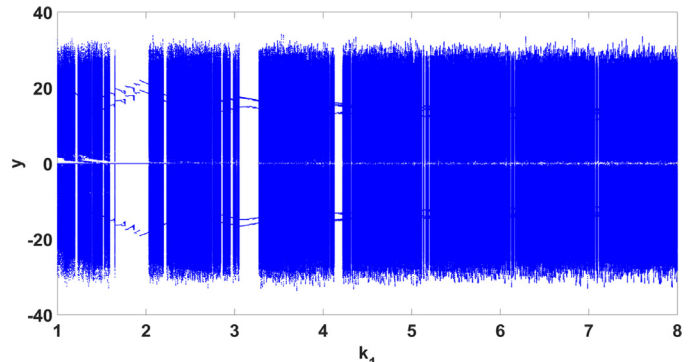


Fig. 16. Bifurcation diagram y vs. k_1 .

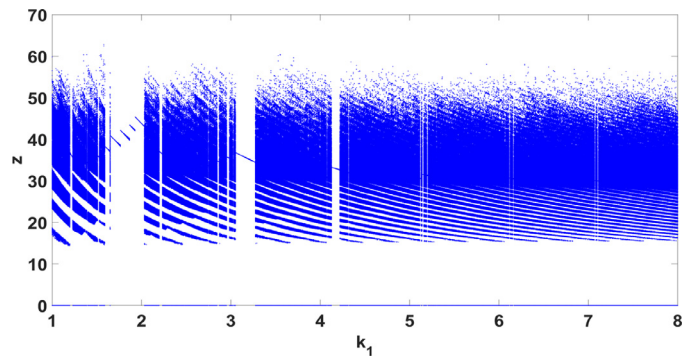


Fig. 17. Bifurcation diagram z vs. k_1 .

found that the outcomes of the bifurcation diagrams are in consistent with the Lyapunov spectrum in Fig. 11.

To know the reflection of increasing value of k_1 on chaoticness of the proposed system, more investigation is carried out on the Lyapunov spectrum of System (2) with respect to k_1 . Now, Lyapunov spectrum is plotted in Fig. 18 by varying k_1 from 1 to 40. This figure shows, there is an increasing trend in the magnitude of positive LE. This property increases the possibility of application of the proposed modified Chen system to many fields. For some more higher values of k_1 , Lyapunov exponents are plotted. For $k_1 = 100$ and $k_1 = 2000$, LES are shown in Fig. 19 and Fig. 20 respectively. These two figures add more clarity on the increasing trend in magnitude of positive LE of the proposed modified Chen system.

Now, a comparison among the largest LE of the proposed system with largest LE of chaotic systems in Yu et al. [20], Li and Hai [29], Huang et al. [32], Wu et al. [35] is listed in Table 2. In these referred papers, the Lyapunov spectra are plotted with respect to different system's parameters, and the largest LE is considered in Table 2.

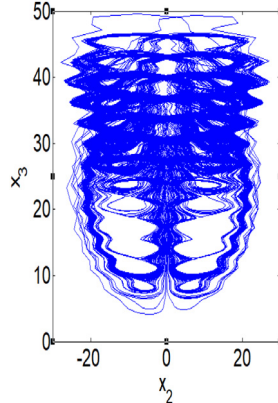
Table 2

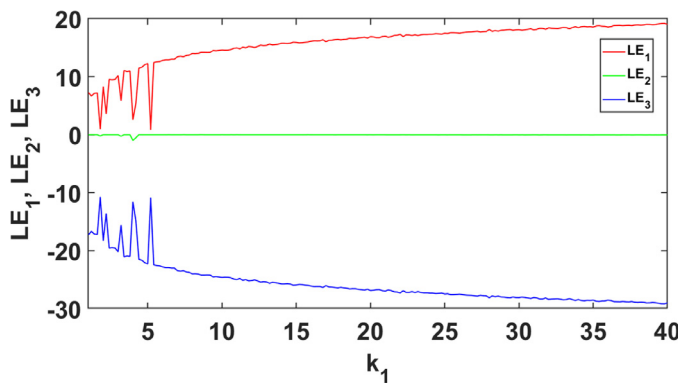
Comparison of the largest LE of the Proposed System with some available similar systems.

References	LLE	Remarks
Proposed system [20]	32.7 0.3	With the increase in value of k_1 , the number of wings as well as the maximum LE is also increasing. the Lyapunov spectrum is plotted with respect to system parameter, k_1 . It is observed that with the increase in value of k_1 , the number of wings increases; however, the maximum LE is not changed.
[29]	1.2	In this article, amplitude modulation and parameter transformation are used to generate multi-wing chaotic attractor. With the variation of the parameter (used for amplitude modulation), the Lyapunov spectrum remains the same.
[32]	2	The number of wings are varied by choosing different set of parameter values. However, with the increase in parameters' value, the maximum LE is not increasing.
[35]	1	A bipolar multi-level pulse signal is used to generate a multi-wing chaotic attractor and the Lyapunov spectrum is plotted with respect to the pulse signal. It is found that with the increase of the magnitude of pulse signal, the largest LE is not increasing.

Table 3

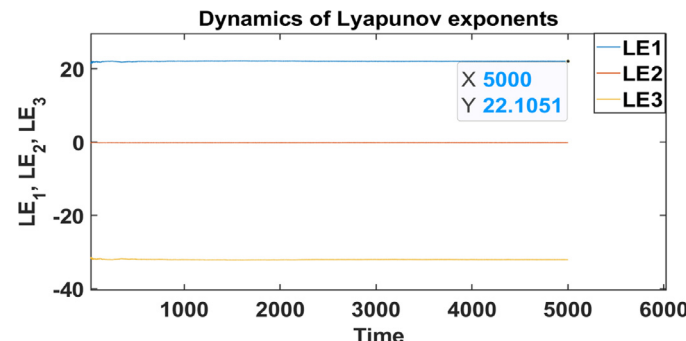
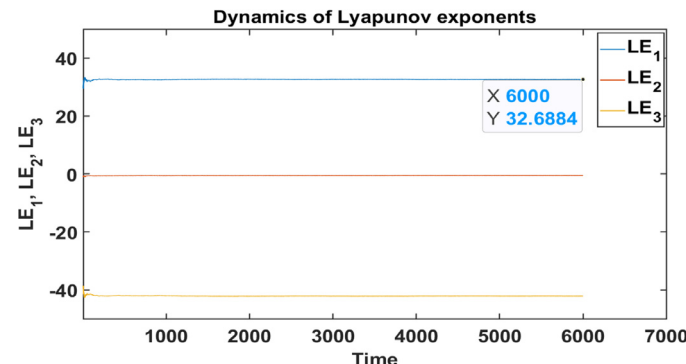
Multi-wing attractors from the two-wing chaotic Lu system.

New systems	System equations with parameters	Lyapunov exponents	Multi-wing attractors
Lu system	$\dot{x} = a(y - x)$, $\dot{y} = cy - xz(1 - k \sin(k_1 z))$, $\dot{z} = -bz + xy$ where $a = 36, b = 3, c = 20, k = 2, k_1 = 2$	LEs of the original Lu system (1.327, 0, -20.33) LEs of the modified Lu system, $k = 2, k_1 = 2$ (6.755, 0, -25.755)	

Fig. 18. Lyapunov spectrum of System (2) with k_1 from 1 to 40..

5. Generation of multi-wings from other two-wing chaotic systems

We were interested to know if the proposed technique is applicable for other two-wing chaotic systems. Thus, the same nonlinear function is multiplied with a nonlinear term of the original Lu [36] system and a multi-wing attractor is generated. The modified Lu system, its parameters, the Lyapunov exponents and the generated multi-wing attractor are given in Table 3. For the modified Lu system, $k = 2$ and $k_1 = 2$ are used to generate the multi-wing attractor. As discussed, the number of equilibrium points can be varied by taking appropriate values of k and k_1 , where k_1 helps to increase or decrease the frequency of the nonlinear function and k is responsible for varying the amplitude of the nonlinear function. Thus, we can generate the desired number of wings from the two-wing Lu system.

Fig. 19. Lyapunov Exponents of System (2) for $k_1 = 100$.Fig. 20. Lyapunov Exponents of System (2) for $k_1 = 2000$.

6. Conclusions

A new design approach to generate a multi-wing chaotic attractor from an available two-wing chaotic attractor is presented. The

proposed design is applied to the Chen system and Lu system, and multi-wing chaotic attractors are successfully generated by varying the designed parameters. The number of wings in the multi-wing attractor can be controlled by varying the designed parameters. Further, the largest Lyapunov exponent of the modified Chen system is comparatively much higher than the original Chen system and can be increased by varying the designed parameters. The proposed multi-wings chaotic systems have much higher largest Lyapunov exponent when compared with four available multi-wing chaotic systems.

The generalisation of the proposed approach for other two-wings chaotic attractor systems requires more investigation and will be taken up in our future research. The concept of recurrent density for counting the number of wings in a chaotic attractor will be considered in our future works [39]. We have used the Wolf algorithm for calculating the Lyapunov exponents. However, there are other algorithms to calculate the Lyapunov exponents. The largest Lyapunov exponent of the modified Chen system is very high using one such algorithm [40]. We are working on it and will report shortly.

Credit author statement

All authors have contributed to the manuscript.

Funding

This research did not receive any specific grant from any funding agency.

Declaration of Competing Interest

Authors declare that they have no conflict of interest.

References

- [1] Mangiarotti S, Peyre M, Zhang Y, Huc M, Roger F, Kerr Y. Chaos theory applied to the outbreak of COVID-19: an ancillary approach to decision-making in pandemic context. *Epidemiol Infect* 2020;148(May). doi:10.1017/S0950268820000990.
- [2] Yu S, Lu J, Chen G. Multifolded torus chaotic attractors: design and implementation. *Chaos* 2007;17(1). doi:10.1063/1.2559173.
- [3] Xiao Y, Sun K, He S. Constructing chaotic map with multi-cavity. *Eur Phys J Plus* 2020;135(1). doi:10.1140/epjp/s13360-019-00052-9.
- [4] Prakash P, Rajagopal K, Singh JP, Roy BK. Megastability, multistability in a periodically forced conservative and dissipative system with signum nonlinearity. *Int J Bifurc Chaos* 2018;28(9):1–10. doi:10.1142/S0218127418300306.
- [5] Hu X, Liu C, Liu L, Yao Y, Zheng G. Multi-scroll hidden attractors and multi-wing hidden attractors in a 5-dimensional memristive system. *Chin Phys B* 2017;26(11). doi:10.1088/1674-1056/26/11/110502.
- [6] Rajagopal K, Bayani A, Jalil A, Khalaf M, Namazi H, Jafari S, Pham V-t. A no-equilibrium memristive system with four-wing hyperchaotic attractor. *AEU-Int J Electron Commun* 2018;95:207–15. doi:10.1016/j.aeue.2018.08.022.
- [7] Wang Z, Ma J, Cang S, Wang Z, Chen Z. Simplified hyper-chaotic systems generating multi-wing non-equilibrium attractors. *Optik* 2016;127(5):2424–31. doi:10.1016/j.jleo.2015.11.099.
- [8] Zhou L, Wang C, Zhou L. A novel no-equilibrium hyperchaotic multi-wing system via introducing memristor. *Int J Circuit Theory Appl* 2018;46(1):84–98. doi:10.1002/cta.2339.
- [9] Zhang X, Wang C. Multiscroll hyperchaotic system with hidden attractors and its circuit implementation. *Int J Bifurc Chaos* 2019;29(9):1–14. doi:10.1142/S0218127419501177.
- [10] Huang L, Zhang Z, Xiang J, Wang S. A new 4D chaotic system with two-wing, four-wing, and coexisting attractors and its circuit simulation. *Complexity* 2019(i). doi:10.1155/2019/5803506.
- [11] Borah M, Roy BK. An enhanced multi-wing fractional-order chaotic system with coexisting attractors and switching hybrid synchronisation with its nonautonomous counterpart. *Chaos, Solitons Fractals* 2017;102:372–86. doi:10.1016/j.chaos.2017.03.055.
- [12] Cui L, Lu M, Ou Q, Duan H, Luo W. Analysis and circuit implementation of fractional order multi-wing hidden attractors. *Chaos, Solitons Fractals* 2020;138. doi:10.1016/j.chaos.2020.109894.
- [13] Yan D, Wang L, Duan S, Chen J, Chen J. Chaotic attractors generated by a memristor-based chaotic system and Julia fractal. *Chaos, Solitons Fractals* 2021;146:110773. doi:10.1016/j.chaos.2021.110773.
- [14] Li N, Susanto H, Cemlyn B, Henning ID, Adams MJ. Secure communication systems based on chaos in optically pumped spin-VCSELs. *Opt Lett* 2017;42(17):3494. doi:10.1364/ol.42.003494.
- [15] Çavuşoğlu Ü, Kaçar S, Pehlivan I, Zengin A. Secure image encryption algorithm design using a novel chaos based S-box. *Chaos, Solitons Fractals* 2017;95:92–101. doi:10.1016/j.chaos.2016.12.018.
- [16] Ge R, Yang G, Wu J, Chen Y, Coatrieux G, Luo L. A novel chaos-based symmetric image encryption using bit-pair level process. *IEEE Access* 2019;7:99470–80. doi:10.1109/ACCESS.2019.2927415.
- [17] Zhu C, Wang G, Sun K. Cryptanalysis and improvement on an image encryption algorithm design using a novel chaos based S-box. *Symmetry* 2018;10(9). doi:10.3390/sym10090399.
- [18] Tang Z, Zhang C, Yu S. Design and circuit implementation of fractional-order multiwing chaotic attractors. *Int J Bifurc Chaos* 2012;22(11):1–10. doi:10.1142/S0218127412502690.
- [19] Zhou L, Wang C, Zhou L. Generating hyperchaotic multi-wing attractor in a 4D memristive circuit. *Nonlinear Dyn* 2016;85(4):2653–63. doi:10.1007/s11071-016-2852-8.
- [20] Yu S, Tang WK, Lü J, Chen G. Design and implementation of multi-wing butterfly chaotic attractors via Lorenz-type systems. *Int J Bifurc Chaos* 2010;20(1):29–41. doi:10.1142/S0218127410025387.
- [21] Hong QQ, Wu Q, Wang X, Zeng Z. Novel nonlinear function shift method for generating multiscroll attractors using memristor-based control circuit. *IEEE Trans Very Large Scale Integr VLSI Syst* 2019;27(5):1174–85. doi:10.1109/TVLSI.2019.2892786.
- [22] Hong Q, Xie Q, Shen Y, Wang X. Generating multi-double-scroll attractors via nonautonomous approach. *Chaos* 2016;26(8). doi:10.1063/1.4959538.
- [23] Liu Y, Guan J, Ma C, Guo S. Generation of $2N + 1$ -scroll existence in new three-dimensional chaos systems. *Chaos* 2016;26(8). doi:10.1063/1.4958919.
- [24] Wang CH, Xu H, Yu F. A novel approach for constructing high-order Chua's circuit with multi-directional multi-scroll chaotic attractors. *Int J Bifurc Chaos* 2013;23(2):1–10. doi:10.1142/S0218127413500223.
- [25] Chen L, Pan W, Wu R, Tenreiro Machado JA, Lopes AM. Design and implementation of grid multi-scroll fractional-order chaotic attractors. *Chaos* 2016;26(8). doi:10.1063/1.4958717.
- [26] Wang Z, Volos C, Kingni ST, Azar AT, Pham VT. Four-wing attractors in a novel chaotic system with hyperbolic sine nonlinearity. *Optik* 2017;131:1071–8. doi:10.1016/j.jleo.2016.12.016.
- [27] Liu J. A four-wing and double-wing 3D chaotic system based on sign function. *Optik* 2014;125(23):7089–95. doi:10.1016/j.jleo.2014.08.095.
- [28] Chen Z, Wen G, Zhou H, Chen J. A new $m \times n$ -grid double-scroll chaotic attractors from rucklidge chaotic system. *Optik* 2017;136:27–35. doi:10.1016/j.jleo.2017.01.088.
- [29] Li C, Hai W. Constructing multiwing attractors from a robust chaotic system with non-hyperbolic equilibrium points. *Automatika* 2018;59(2):184–93. doi:10.1080/0005144.2018.1516273.
- [30] Yu N, Wang YW, Liu XK, Xiao JW. 3D Grid multi-wing chaotic attractors. *Int J Bifurc Chaos* 2018;28(4):1–16. doi:10.1142/S0218127418500451.
- [31] Ali AM, Ramadhan SM, Tahir FR. A novel 2D-grid of scroll chaotic attractor generated by CNN. *Symmetry* 2019;11(1):1–11. doi:10.3390/sym11010099.
- [32] Huang Y, Zhang P, Zhao W. Novel grid multiwing butterfly chaotic attractors and their circuit design. *IEEE Trans Circuits Syst II* 2015;62(5):496–500. doi:10.1109/TCSII.2014.2385274.
- [33] Huang Y. A novel method for constructing grid multi-wing butterfly chaotic attractors via nonlinear coupling control. *J Electr Comput Eng* 2016. doi:10.1155/2016/9143989.
- [34] Zhang C, Yu S. On constructing complex grid multi-wing hyperchaotic system: theoretical design and circuit implementation. *Int J Circuit Theory Appl* 2013;41(3):221–37.
- [35] Wu Q, Hong Q, Liu X, Wang X, Zeng Z. Constructing multi-butterfly attractors based on Sprott C system via non-autonomous approaches. *Chaos* 2019;29(4). doi:10.1063/1.5087976.
- [36] Yu S, Tang WK, Lü J, Chen G. Generating 2N-wing attractors from Lorenz-like systems. *Int J Circuit Theory Appl* 2010;38(3):243–58. doi:10.1002/cta.558.
- [37] Singh JP, Roy BK. The nature of Lyapunov exponents is $(+, -, -)$. Is it a hyperchaotic system? *Chaos, Solitons Fractals* 2016;92:73–85. doi:10.1016/j.chaos.2016.09.010.
- [38] Singh JP, Roy BK. A more chaotic and easily hardware implementable new 3-D chaotic system in comparison with 50 reported systems. *Nonlinear Dyn* 2018;93(3):1121–48. doi:10.1007/s11071-018-4249-3.
- [39] Tutueta AV, Butusov DN, Karimov AI, Andreev VS. Recurrence density analysis of multi-wing and multi-scroll chaotic systems. In: 2018 7th Mediterranean conference on embedded computing, MECO 2018 – including ECYPS 2018, proceedings, vol. 1; 2018. p. 1–5. doi:10.1109/MECO.2018.8406087.
- [40] Mendes EM, Nepomuceno EG. A very simple method to calculate the (positive) largest Lyapunov exponent using interval extensions. *Int J Bifurc Chaos* 2016;26(13):1–7. doi:10.1142/S0218127416502266.